Manuscript refereed by Prof Herbert Danninger (Vienna Technical University, Austria)

Enhancement of Fatigue-Properties of MIM-Processed Ti-6Al-4V by Addition of Yttrium and Characterization by In Situ X-Ray Scattering

W. Limberg, R. Willumeit-Römer, F. Pyczak, T. Ebel, A. Stark (Helmholtz-Zentrum Geesthacht, Zentrum für Material- und Küstenforschung GmbH, Institute of Materials Research, Max-Planck-Straße 1, 21502 Geesthacht, Germany) wolfgang.limberg@hzg.de regine.willumeit@hzg.de florian.pyczak@hzg.de thomas.ebel@hzg.de andreas.stark@hzg.de

Abstract

In this study fatigue and tensile test specimens were produced by Metal Injection Moulding (MIM) using gas atomised Ti-6Al-4V-powder with addition of 0.5 wt.% yttrium powder as well as pure Ti-6Al-4V-powder as reference. The addition of yttrium resulted in a noticeably refinement of the grain size from 150 µm to 50 µm by formation of Y_2O_3 particles hindering grain growth. Corresponding scavenging of oxygen from the titanium matrix led to a decrease in tensile strength of about 70 MPa. Surprisingly, fatigue strength was enhanced by 15 to 60 MPa, probably caused by the colony refinement overcompensating the effect of decreased yield strength. To understand the formation kinetics of Y_2O_3, in situ X-ray diffraction experiments were performed during sintering using synchrotron radiation. The results show that only a small amount of yttrium was dissolved while the remainder was oxidized. The formation of Y_2O_3 took place between 850 and 1050 °C.

Introduction

A fine microstructure is very important for good mechanical properties at room temperature, for statically loaded parts as well as for parts under dynamic load. MIM is a near net shape production technique with sintering, as a heat treatment at high temperature, as last integrated production step. Thus, the possibilities of microstructural refinement of MIM-processed α-β-titanium alloys like Ti-6Al-4V are limited compared to thermomechanically treated material. One possibility to get a fine microstructure is to apply thermo-hydrogen processing (THP) after sintering [1, 2]. But this post processing needs special furnace equipment and exact control of temperature and hydrogen partial pressure. An easier way to achieve a fine microstructure is the addition of a small amount of boron powder (0.5 wt.-%) to the Ti-6Al-4V-MIM-Feedstock. This leads to a strong colony refinement, excellent tensile strength and very good fatigue resistance [3]. Another strong colony refining agent is yttrium oxide. The colony size of MIM-processed Ti-6Al-4V can be reduced from initially 130 µm down to 50 µm by addition of only 0.1 wt. % Y_2O_3 [4]. An important parameter, which influences the mechanical properties of titanium materials, is the oxygen content. A small amount of additional oxygen provides higher tensile strength, but it leads to a strong decrease in ductility when the critical value of about 0.32 wt.-% in the case of Ti-6Al-4V is exceeded [3, 5, 6].

When pure elementary yttrium is added to Ti-6Al-4V instead of Y_2O_3, the Y_2O_3 is formed in-situ during the sintering process. Scavenging oxygen from the titanium matrix takes place, increasing ductility, and the formed Y_2O_3 particles lead to colony refinement. In the last two decades there was an increasing interest in the use of rare earth based materials to mitigate the detrimental effect of oxygen on ductility [7, 8]. Due to the very low amount of rare earth elements which are already sufficient for colony refinement, the additional costs should be balanced by the possibility to use cheaper lower quality powder.

Y_2O_3 is one of the most stable oxides. Because of this high stability it is normally used as coating material for furnace plates which are in direct contact with titanium at elevated temperatures. So normally no strong interaction between titanium and Y_2O_3 should be assumed. One of the most interesting questions is the reason of the observed colony refinement, especially which phases are formed at the interface between Y_2O_3 and titanium (e. g. yttrium titanates $Y_2Ti_2O_7$ and Y_2TiO_5).

Furthermore it is of interest at which temperatures the Y_2O_3 is formed. If the forming temperature of Y_2O_3 is significant higher than the temperature of yttrium solution in titanium, it's another indication for the scavenging of oxygen by yttrium. Therefore, the aim of this study is to observe the kinetics of solution of yttrium and formation of Y_2O_3 during sintering of Ti-6Al-4V and to investigate the influence of yttrium addition on the fatigue properties.

Experimental Details

Powders. The Ti-6Al-4V alloy powder (Fig. 1a) used for these experiments was a plasma atomised Grade 5 powder produced by AP&C in Quebec, Canada. The used powder fraction had a particle diameter < 45 µm. The powder particles are spherically shaped with a smooth surface, which is beneficial for the injection moulding process.

The yttrium powder (Fig. 1b) is commercial available powder with a purity of >99.9 %, purchased by Stanford Advanced Materials, Irvine, CA 92618 USA. The shape of the yttrium powder particles is square-edged with a rough cracky surface. It was delivered with a particle size < 80 µm (Mesh 200). The fine powder fraction < 32 µm was extracted from the powder by sieving. The initial oxygen content of the yttrium powder has been determined to 0.9 wt.-%.

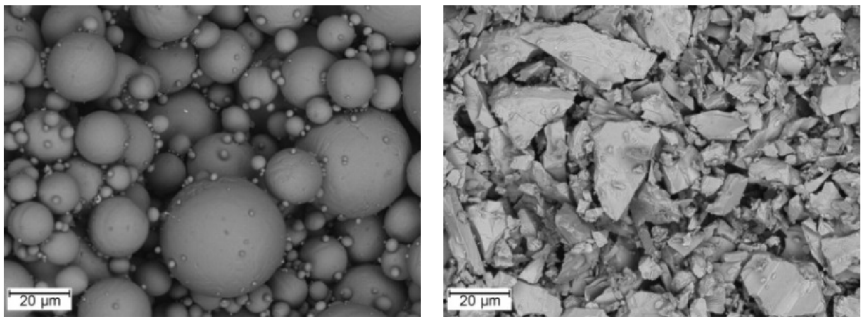

a) Ti-6Al-4V *b) Yttrium*

Fig. 1 SEM images of the used powders

Feedstock preparation. The binder used is the same, as also applied by the authors for MIM of conventional titanium alloys which exhibit good mechanical properties of the sintered specimens [9]. It is a mixture of ethylene vinyl acetate (EVA), paraffin wax (PW) and stearic acid (SA).

The entire powder handling was performed in a glove box under argon atmosphere to prevent the fine powder from further oxidation. The residual oxygen in the argon atmosphere was eliminated by a gas purifier, so the oxygen content in the glove box could be kept below 1 ppm. At first, the Ti-6Al-4V powder and the yttrium powder were blended in a planetary mixer for four minutes at a speed of 2000 min^{-1} to break up particle clusters and achieve a homogeneous dispersion. The feedstock, which contains 10 wt.% (35 vol.%) of binder, was prepared by mixing Ti-6Al-4V alloy powder, yttrium powder and binder in a double Z-blade mixer (Femix KM 0,5 K) for two hours at a temperature of 120 °C. After solidification, the feedstock was granulated by means of a cutting mill.

Three different feedstocks were produced (all containing 10 wt.-% of binder):

1. Pure Ti-6Al-4V
2. Ti-6Al-4V + 0.2 wt.-% Y powder
3. Ti-6Al-4V + 0.5 wt.-% Y powder

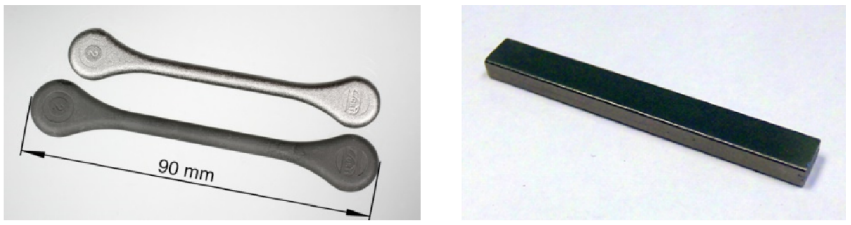

a) MIM tensile test specimens in accordance to ISO 2740 (sintered and green part).

b) Rectangular block specimen for four point bending fatigue tests

Fig. 2 MIM-produced specimens

Injection moulding. For tensile tests, standard MIM specimens according to ISO 2740 (Fig. 2a) were injection moulded, using a two-cavity mould on a conventional ARBURG 320 S 500-60 machine. An injection pressure of 800 bar, an injection rate of 35 cm^3/s, an injection temperature of 112 °C and a mould temperature of 43 °C turned out to be adequate parameters for the injection process. For fatigue tests in four-point bending mode, rectangular block specimens (Fig. 2b) with green part dimensions 50 mm x 6.3 mm x 3.4 mm were injection moulded.

Fatigue tests. Prior to the fatigue testing, the rectangular block specimens were surface treated by shot peening to minimize the influence of surface defects. The used blasting medium was spherical zirconium oxide with a particle diameter between 125 and 425 µm. The shot peening was conducted on a conventional air-blast machine with an air pressure of 8 bar, a nozzle diameter of 6.5 mm and a working distance of 30 mm. The fatigue tests were conducted in air at room temperature on a RUMUL resonance testing machine Mikrotron 654-H with a cyclic frequency of 95 Hz at a load ratio $R = \sigma_{min}/\sigma_{max}$ of 0.2.

Tensile tests. The tensile tests according to ISO 6892-1 were done in air at room temperature on a Schenck Trebel RM 100 tensile testing machine with a crosshead speed of 0.5 mm/min. The gauge length was 30 mm and the gauge diameter 4.3 mm. The strain was measured by a laser extensometer (Fiedler Laser Scanner). All tensile test specimens were tested in the as-sintered condition.

Characterisation techniques. For microscopy investigations the samples were embedded in artificial resin and mechanically ground and polished. The microstructures were observed by SEM using back scattered electron (BSE) imaging and electron backscatter diffraction (EBSD) patterns were used for determining the colony size. The chemical compositions were measured by energy dispersive X-ray (EDX) analysis, and the density of the specimens was determined by buoyancy in ethanol. To calculate the porosities, the densities were compared to the density of a non-porous MIM Ti-6Al-4V specimen which was additionally hot isostatic pressed (4.42 g/cm^3)**.**

In situ synchrotron X-ray diffraction. For the in situ diffraction experiments cylindrical specimens were prepared out of the gauge region of the tensile test samples. The diameter of the cylindrical specimens was 5 mm and the length between 11 and 13 mm. After debinding, the specimens were pre-sintered at a temperature of 850 °C for 30 minutes, to achieve a sufficient mechanical stability for further handling. The porosities of the pre sintered specimens were between 25 and 30 %. For temperature control, a PtRh/Pt thermocouple has been fixed at the surface of the specimens by resistance spot welding. This direct contact is necessary, because the specimen is heated by electromagnetic induction. Only the pure Ti-6Al-4V and the Ti-6Al-4V with addition of 0.5 wt.-% Y powder were investigated by synchrotron X-ray diffraction.

The X-ray diffraction experiments were done at the German Electron Synchrotron (DESY) PETRA III at the beamline P07 [10] in a dilatometer DIL 805A/D (TA Instruments formerly Bähr), especially modified for X-ray diffraction [11]. High-energy X-rays with an energy of 100 keV, a wave length of 12.4 pm and a spot size of 1mm x 1mm were used for the diffraction experiments. The specimens were heated up to 800 °C with a heating rate of 50 °C/min and above 800 °C with a heating rate of 5 °C/min. The sintering was performed in vacuum of 2 x 10^{-5} mbar. During heating the diffraction patterns were recorded every 10 s on a PerkinElmer XRD 1622 flat panel detector with an exposure time of 0.1 sec. Diffraction diagrams were generated from the detector images using the Fit2D image analysing Software [12]. The peaks of the diffraction diagrams were identified using Pearson's Crystal Data - Crystal Structure Database for Inorganic Compounds.

During heating, a eutectic reaction occurred between the platinum of the thermocouple and the aluminium of the Ti-6Al-4V alloy, which led to a liquid phase formation at the contact area between specimen and thermocouple and thereby a detachment of the thermocouple from the specimen. This happened between 1300 and 1380 °C before the dwell temperature of 1400 °C could be reached and led to the termination of the experiments.

Results and discussion

Microstructure and porosity. Fig. 3 shows SEM images (BSE-mode) of cross-sections of the sintered tensile test specimens of Ti-6Al-4V with and without addition of yttrium powder. The microstructure consists of lamellar α/β colonies. The α-lamellae appear dark grey while the β-phase between the α-lamellae is visible in a light grey colour. The pores are visible as black dots. EDX and X-ray diffraction experiments have shown that the white structures are Y_2O_3 particles which were formed during the sintering process.

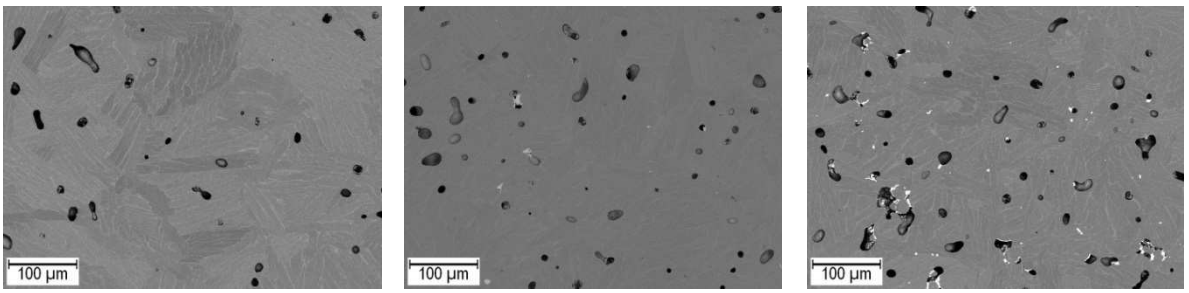

a) Ti-6Al-4V b) Ti-6Al-4V + 0.2 wt.-% Y c) Ti-6Al-4V + 0.5 wt.-% Y

Fig. 3 SEM (BSE-mode) micrographs of MIM processed Ti-6Al-4V with different yttrium powder additions

The pores of the pure Ti-6Al-4V and the Ti-6Al-4V with addition of 0.2 wt.-% yttrium are homogeneously distributed, only the specimens with addition of 0.5 wt.-% Y show a few pore clusters with sizes up to 100 µm, partially filled with Y_2O_3. The residual porosities of the different specimens

are listed in Table 1. The porosity of the pure Ti-6Al-4V specimens with 3.5 % is a little bit higher than expected. Sintering in the furnace with similar alloys at 1400 °C under good vacuum conditions normally results in porosities which are slightly below 3 %. Obviously, the porosity increases with the addition of yttrium. This is also in accordance with earlier investigations where coarser yttrium powders were used [13].

Because of the irregular shape of the colony boundaries, the usage of the linear intercept method to determine the colony size leads to abnormally low values. A better way to determine the colony sizes of such alloys is to use EBSD-patterns, determine the average colony area Ā by image analysis and calculate the average mean colony diameter by taking the square root of Ā.

Fig. 4 shows EBSD-patterns of cross-sections of MIM processed Ti-6Al-4V and Ti-6Al-4V with 0.5 wt.-% yttrium powder addition, respectively. The areas with different colours are α/β colonies with different orientation. Such images are well suited to determine the colony sizes of the different specimens. The two images 100 µm, partially filled with Y_2O_3. The residual porosities of the different specimens

at the outside (a1 and b2) show the differently oriented α-colonies of the Ti-6Al-4V specimen. The initial colony size was measured as 125 µm in average. A decrease in average colony size from 125 to 90 µm by adding 0.5 wt.-% yttrium was found.

The two images in the centre of Fig. 4 (a2 and b1) show the regions of differently oriented β-phase between the α-lamellae. For better visibility, the contrast of the images has been enhanced and the fields with different orientation were separated by red lines. The β-phase images show the same regions as the α-phase images. Since the α-lamellae grow into the β-grains during cooling after sintering, the β-phase images in Fig. 4 represent the size of the prior β-grains. Obviously the addition of yttrium powder hinders the growth of β-grains during the sintering of Ti-6Al-4V. The prior β-grain size of the Ti-6Al-4V samples was determined as 235 µm. By addition of 0.5 wt.-% yttrium, the prior β-grain size decreases to 175 µm.

The decrease in colony size of Ti-6Al-4V by addition of 0.5 wt.-% yttrium is 28 %, this is the same difference as between the prior β-grain sizes. This leads to the conclusion that the colony refinement is mainly caused by the hindering of β-grain growth and not by heterogeneous nucleation of α-lamellae.

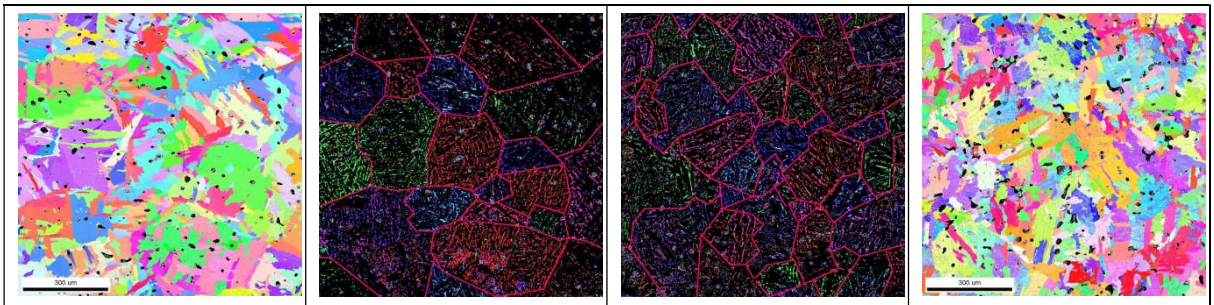

a1) α-phase | *a2*) β-phase | *b1*) β-phase | b2) α-phase

a) Ti-6Al-4V b) Ti-6Al-4V + 0.5 wt.-% Y

Fig. 4 EBSD-patterns of MIM processed Ti-6Al-4V and Ti-6Al-4V with 0.5 wt.-% yttrium

Impurity levels. The concentrations of oxygen and nitrogen of the alloy powder (powder particle diameter < 45 µm) and of the MIM-manufactured specimens after sintering were analysed. The impurity levels of the various MIM specimens are listed in Table 1. While the alloy powder had an initial oxygen content of 1600 µg/g, it increased to 2356 µg/g during sintering at 1400 °C. So the increase in oxygen content of pure Ti-6Al-4V during the MIM-processing is about 750 µg/g, which is comparatively high as experience shows. Under optimised conditions, the increase during MIM-processing can be limited to 350 µg/g [13, 14]. This high oxygen pick up could be one reason for the low colony sizes and the high porosities. Compared to the sintered yttrium-free specimen a further increase of 24 µg/g of oxygen for 0.2 %, and 145 µg/g of oxygen for 0.5 % yttrium is found in the yttrium containing sintered specimens. Based on these results it is possible to estimate the

Specimen composition		YS [MPa]	UTS [MPa]	ε_f [%]	Porosity [%]	Oxygen content [µg/g]	Nitrogen content [µg/g]
Initial Powder						1600	200
Ti-6Al-4V		771	884	15.3	3.5	2356 ± 78	501 ± 104
Ti-6Al-4V + Y	0.2 wt.-%	739	849	13.2	4.3	2380 ± 76	536 ± 24
	0.5 wt.-%	692	794	12.5	5.0	2501 ± 94	590 ± 72

Table 1 Mechanical properties, porosity and impurity contents of MIM-processed Ti-6Al-4V

effectiveness of the oxygen scavenging effect. Taking the stoichiometry of Y_2O_3 and the atomic masses of oxygen and yttrium into account (16 for oxygen and 89 for yttrium) the 0.5 wt.-% of yttrium added to the alloy need 0.135 wt.-% oxygen to fully transform to Y_2O_3. This results in 1350 µg/g oxygen content in the alloy which is bound to yttrium in the form of oxide. Only a minor part of this oxygen was introduced into the alloy mixture with the yttrium powder (145 µg/g for 0.5 % yttrium) and nearly 90% of the oxygen now bound as oxide was scavenged from the titanium matrix by yttrium.

Tensile test properties. The results of the tensile tests are listed in Table 1. The MIM-processed specimens of pure Ti-6Al-4V sintered at 1400 °C showed a yield strength (YS) of 771 MPa, an ultimate tensile strength (UTS) of 884 MPa and a plastic elongation (ε_f) of 15.3 %, which are common values for MIM-Ti-6Al-4V with the applied binder system and process parameters [13]. The addition of yttrium leads to a decrease of UTS, YS and ε_f. The decrease in strength could be caused by a reduced oxygen content of the titanium matrix due to the scavenging effect of yttrium but also, at least partially, by the increase of porosity. For an increase in porosity of 1.5 % a decrease in ultimate tensile strength of approximately 35 MPa has been observed in former investigations at MIM-processed Ti-6Al-4V [15]. That means that from the decrease of 90 MPa by addition of 0.5 wt.-% yttrium to Ti-6Al-4V, 35 MPa are caused by the increased porosity and 55 MPa are caused by the oxygen reduction due to the scavenging effect.

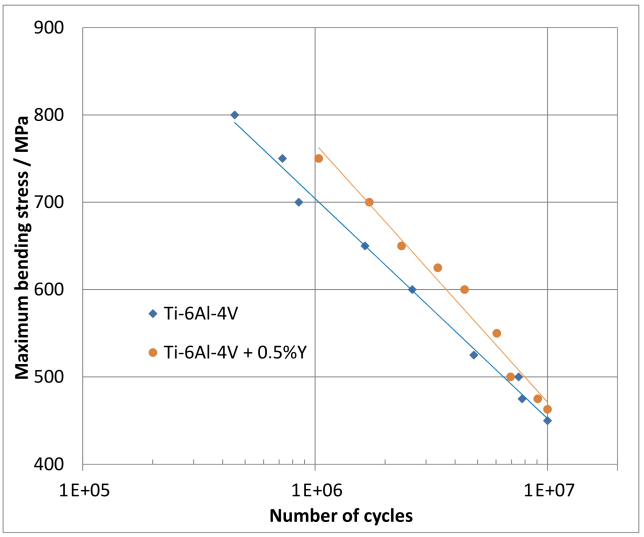

Fig. 5 Fatigue properties of MIM-Ti-6Al-4V and MIM-Ti-6Al-4V with addition of 0.5 wt.-% yttrium (R = 0.2)

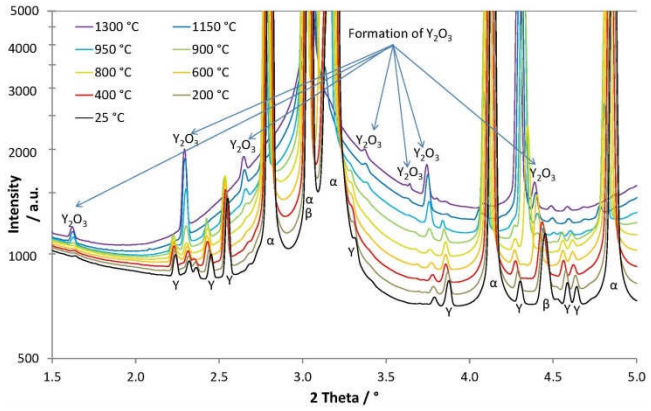

Fig. 6 X-Ray diffraction diagrams of Ti-6Al-4V with addition of 0.5 wt.-% yttrium at different temperatures

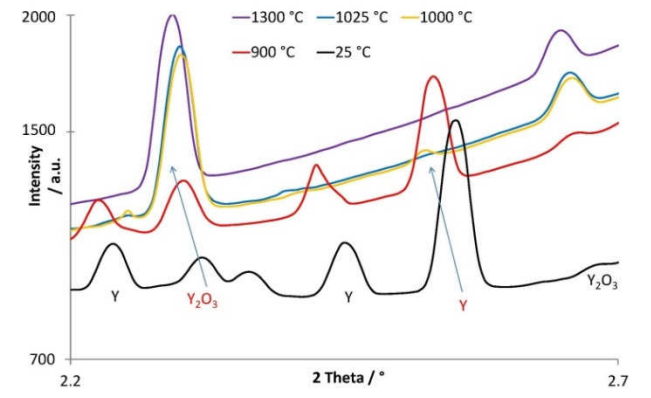

Fig. 7 2Θ-region between 2.2 and 2.7 ° of X-Ray diffraction diagrams of MIM-Ti-6Al-4V with addition of 0.5 wt.-% yttrium

Fatigue properties. The results of the fatigue experiments are shown in Fig. 5. For pure Ti-6Al-4V, the fatigue strength at 10^7 cycles is 450 MPa, which is the same value as found by O. Ferri [16] for this alloy. Contrary to the tensile tests, the addition of 0.5 wt.-% yttrium increases the fatigue strength at 10^7 cycles from 450 to 470 MPa. At lower numbers of load cycles (10^6), the fatigue strength even increases from 705 to 765 MPa. So the colony size seems to have more influence on the fatigue behaviour than the porosity or the oxygen content, at least at oxygen values which do not lead to embrittlement.

Synchrotron X-ray diffraction. Fig. 6 shows the diffraction diagrams of Ti-6Al-4V with addition of 0.5 wt.-% yttrium taken at different temperatures during heating up. With increasing temperature, all peaks shift to lower values of 2Θ which is caused by the thermal expansion of the lattice. The intensity of the main Y_2O_3-peak at 2Θ = 2.3 ° shows a strong increase between 800 and 900 °C. Thus, in this temperature range the formation of Y_2O_3 accelerates.

Fig. 7 shows the 2Θ-region between 2.2 and 2.7 °, where the peaks of yttrium and Y_2O_3 with the highest intensity (labelled in red) are located. A small amount of yttrium is already oxidised during or before the pre-sintering. The main yttrium-peak at 2Θ = 2.5 ° disappears between 1000 and 1025 °C, which means all yttrium is dissolved in the titanium matrix or oxidised and no elemental yttrium is present any more at 1025 °C.

In the same temperature range, the main Y_2O_3-peak at 2Θ = 2.3 ° reaches its highest intensity which then stays constant up to 1300 °C. This means, that there is no further oxidation of yttrium above 1025 °C and only a small amount of yttrium was dissolved before oxidation.

No formation of yttrium titanates as $Y_2Ti_2O_7$ or Y_2TiO_5 was observed. This should be part of further investigations i.e. by transmission electron microscopy of the interface between Y_2O_3-particles and the Ti-6Al-4V matrix.

Conclusions

- Yttrium hinders the growth of β-grains during the sintering of Ti-6Al-4V.
- The addition of yttrium to MIM-processed Ti-6Al-4V did not enhance the tensile strength by colony refinement, most probably due to the oxygen scavenging effect.
- Contrary to the tensile test behaviour, the fatigue strength of MIM-processed Ti-6Al-4V increased with addition of 0.5 wt.-% yttrium.
- Only a small amount of yttrium was dissolved before oxidation.
- No yttrium titanates like $Y_2Ti_2O_7$ and Y_2TiO_5 could be observed by synchrotron X-ray diffraction.

References

1. Paramore, J.D., Z. Zak Fang, and P. Sun, Hydrogen sintering of titanium and its alloys, in Titanium Powder Metallurgy, F.H. Froes, Editor. 2015, Butterworth-Heinemann: Boston. p. 163-182.
2. Qazi, J.I., et al., Kinetics of martensite decomposition in Ti–6Al–4V–xH alloys. Materials Science and Engineering: A, 2003. 359(1–2): p. 137-149.
3. Ferri, O.M., T. Ebel, and R. Bormann, The Influence of a Small Boron Addition on the Microstructure and Mechanical Properties of Ti-6Al-4V Fabricated by Metal Injection Moulding. Advanced Engineering Materials, 2011. 13(5): p. 436-447.
4. Limberg, W., T. Ebel, and K.U. Kainer. Addition of Rare Earth Elements to MIM-processed TiAl6V4. in Proc. Euro PM2014. 2014. Salzburg (A): EPMA. Paper no. EP140185.
5. Miura, H., H.G. Kang, and Y. Itoh, High Performance Titanium Alloy Compacts by Advanced Powder Processing Techniques. Key Engineering Materials, 2012. 520: p. 30-40.
6. Ebel, T., et al., Metal Injection Moulding of Titanium and Titanium-Aluminides. Key Engineering Materials, 2012. 520: p. 153-160.
7. Yan, M., H.P. Tang, and M. Qian, Scavenging of oxygen and chlorine from powder metallurgy (PM) titanium and titanium alloys, in Titanium Powder Metallurgy, F.H. Froes, Editor. 2015, Butterworth-Heinemann: Boston. p. 253-276.
8. Yang, Y.F., et al., Impurity scavenging, microstructural refinement and mechanical properties of powder metallurgy titanium and titanium alloys by a small addition of cerium silicide. Materials Science and Engineering A, 2013. 573 p. 166-174.
9. Obasi, G.C., et al., Influence of processing parameters on mechanical properties of Ti–6Al–4V alloy fabricated by MIM. Materials Science and Engineering: A, 2010. 527(16–17): p. 3929-3935.
10. Schell, N., et al., The High Energy Materials Science Beamline (HEMS) at PETRA III. Materials Science Forum, 2014. 772: p. 57-61.
11. Staron, P., et al., In Situ Experiments with Synchrotron High-Energy X-Rays and Neutrons. Advanced Engineering Materials, 2011. 13 (8): p. 658-663.
12. Hammersley, A.P., et al., Two-dimensional detector software: From real detector to idealised image or two-theta scan. High Pressure Research, 1996. 14(4-6): p. 235-248.
13. Limberg, W. and T. Ebel, Metal Injection Moulding of Ti-6Al-4V with Yttrium Addition, in Key Engineering Materials. 2016. p. 20-27.
14. Ebel, T., et al., Metal injection molding of titanium, in Titanium Powder Metallurgy, F.H. Froes, Editor. 2015, Butterworth-Heinemann: Boston. p. 337-360.
15. Ebel, T., et al. MIM fabrication of porous Ti-6Al-4V components for biomedical application. in Proc. Euro PM2010. 2010. Florence (I): EPMA. p. 797-804.
16. Milagres Ferri, O., Optimisation of Fatigue Behaviour of Ti-6Al-4V Alloy Components Fabricated by Metal Injection Moulding. 2010. PhD thesis. Technische Universität Hamburg-Harburg.